Supporting Information

A Potentially General Approach to Aliphatic Ester-Derived PVC Plasticizers with Suppressed Migration as Sustainable Alternatives to DEHP

Siyu Pan[1], Delong Hou[2], Jinming Chang[3], Zhou Xu[4], Songhang Wang[2], Sunxian Yan[2], Qi Zeng[1], Zhonghui Wang[2], Yi Chen[1,5,*]

[1] *College of Biomass Science and Engineering, Sichuan University, Chengdu 610065, P.R. China*

[2] *Key Laboratory of Leather Chemistry and Engineering of Ministry of Education, Sichuan University, Chengdu 610065, P.R. China*

[3] *Chemical Synthesis and Pollution Control Key Laboratory of Sichuan Province, China West Normal University, Nanchong 637009, P.R. China*

[4] *School of Life Science and Food Engineering, Yibin University, Yibin 644007, P.R. China*

[5] *Department of Chemistry, Massachusetts Institute of Technology, Cambridge, Massachusetts, 02139, United States*

* Corresponding author. *E-mail address:* chenleon@mit.edu

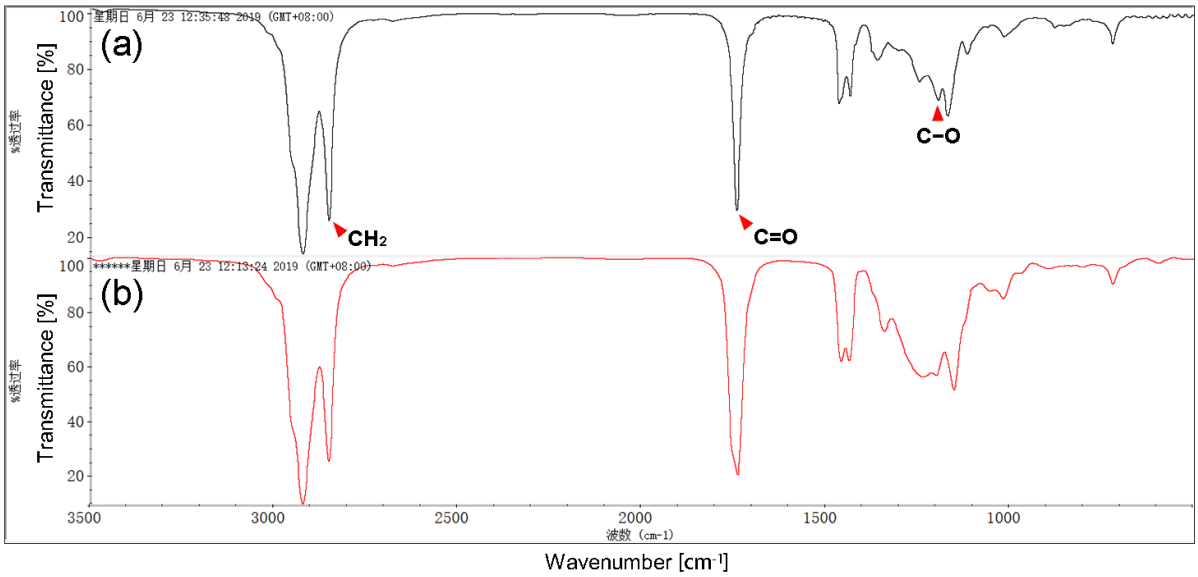

Figure S1. FT-IR spectra of (a) MS and (b) EB-MS. Relative to MS, the absorption intensity ratios of carbonyl (1745 cm^{-1}) and C-O (1196 cm^{-1}) stretching to that of methylene (2854 cm^{-1}) increased from 0.89 and 0.29 to 1.15 and 0.4, respectively, after Claisen condensation. Methylene were selected as the internal standard for quantitative comparison as they remained stoichiometrically consistent throughout the functionalization procedure.

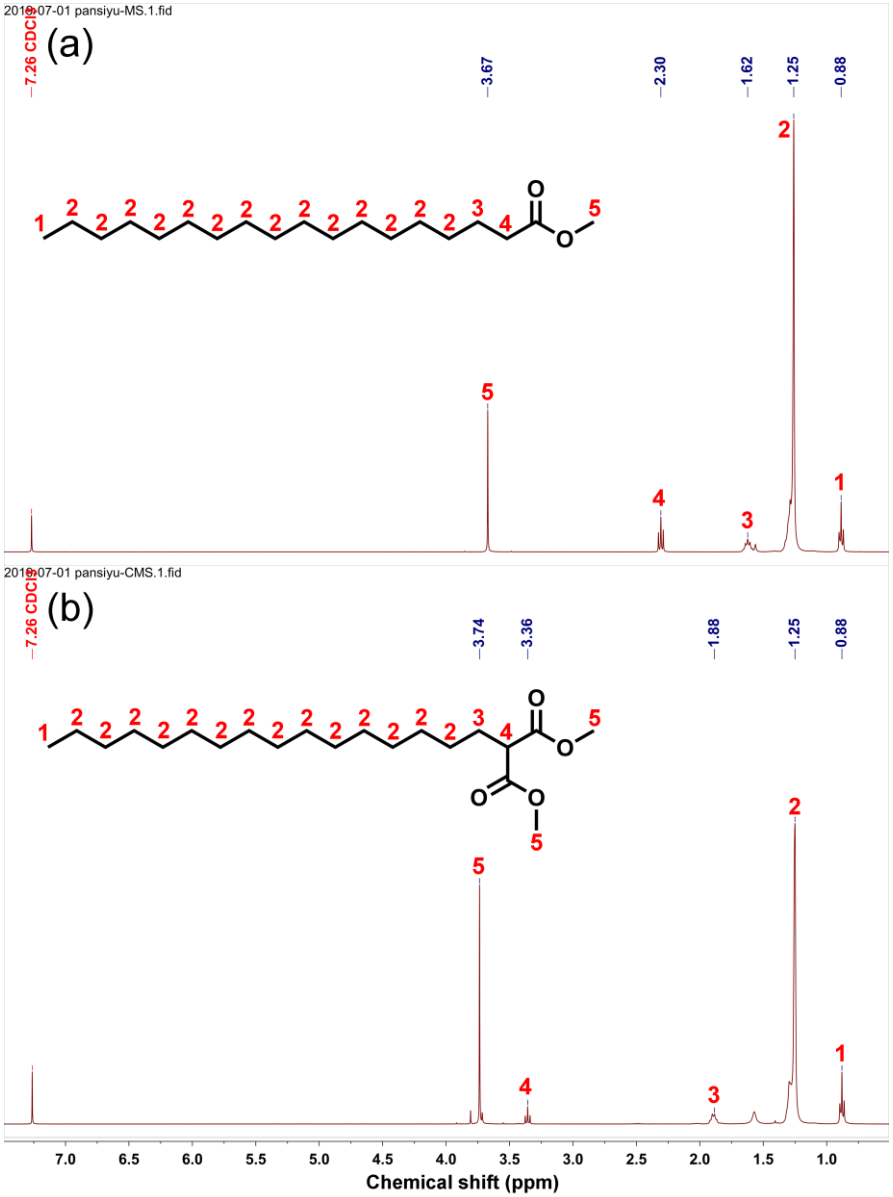

Figure S2. ^{1}H NMR spectra of (a) MS and (b) EB-MS. Relative to the signal corresponding to methyl protons (**1**) whose position and integral remained constant before and after Claisen condensation, the integral under the methoxy resonance signal (**5**) doubled in EB-MS, suggesting those extra methyl esters were in stoichiometric quantities. One could surmise that the ester branch was covalently attached at the α-position of the feedstock, given the integral under the α-proton signal (**4**) was halved after Claisen condensation. Meanwhile, the attached ester thinned the electron clouds on adjacent protons, and hence the resonance position of the α- (**4**) and β-protons (**3**) shifted downfield from 2.3 and 1.6 to 3.4 and 1.9 ppm, respectively. Despite a decrease in signal height, the integral under the methylene protons (**2**) remained almost unchanged before and after Claisen condensation.

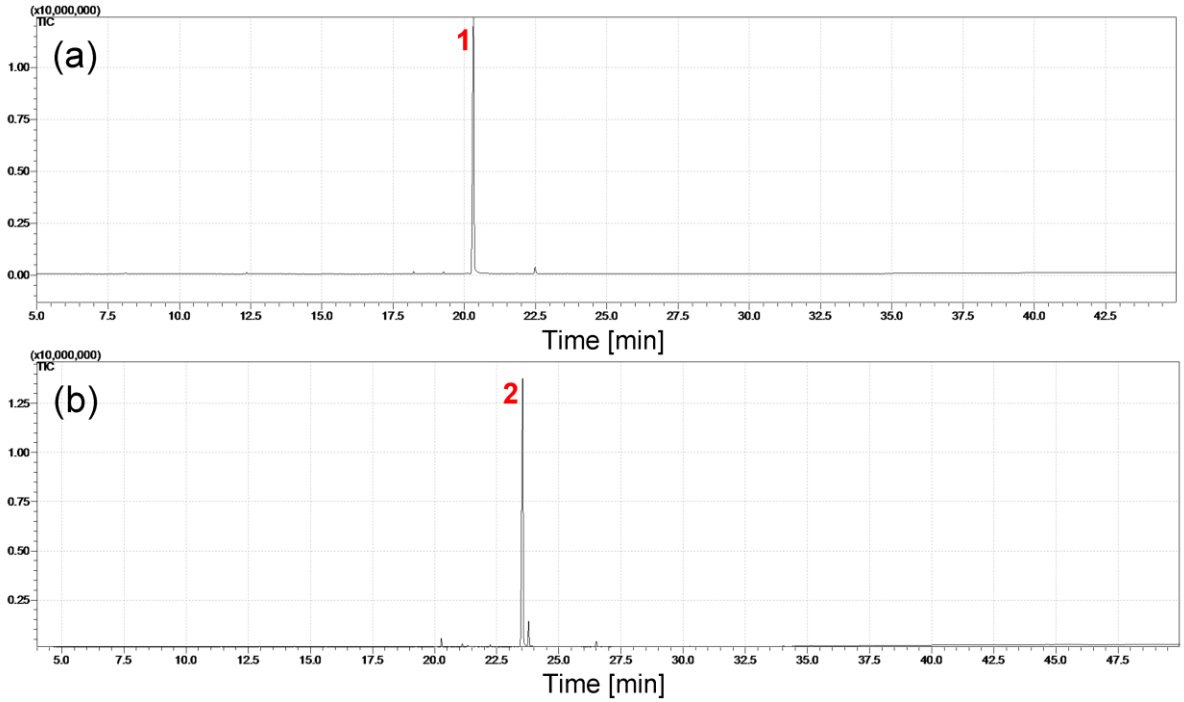

Figure S3. Gas chromatograms of (a) MS and (b) EB-MS.

Table S1. Composition of each gas chromatogram peak in Figure S3 as identified by comparing their recorded mass spectra against NIST08 Mass Spectral Library.

Peak	Retention time (min)	Component	Molecular formula	Area (%)		Matching degree (%)
				Feedstock	Product	
1	20.3	Methyl stearate	$C_{19}H_{38}O_2$	96.6		95
2	23.6	Ester-branched methyl stearate	$C_{21}H_{40}O_4$		89.1	94
		Other compounds	n/a	3.4	10.9	n/a

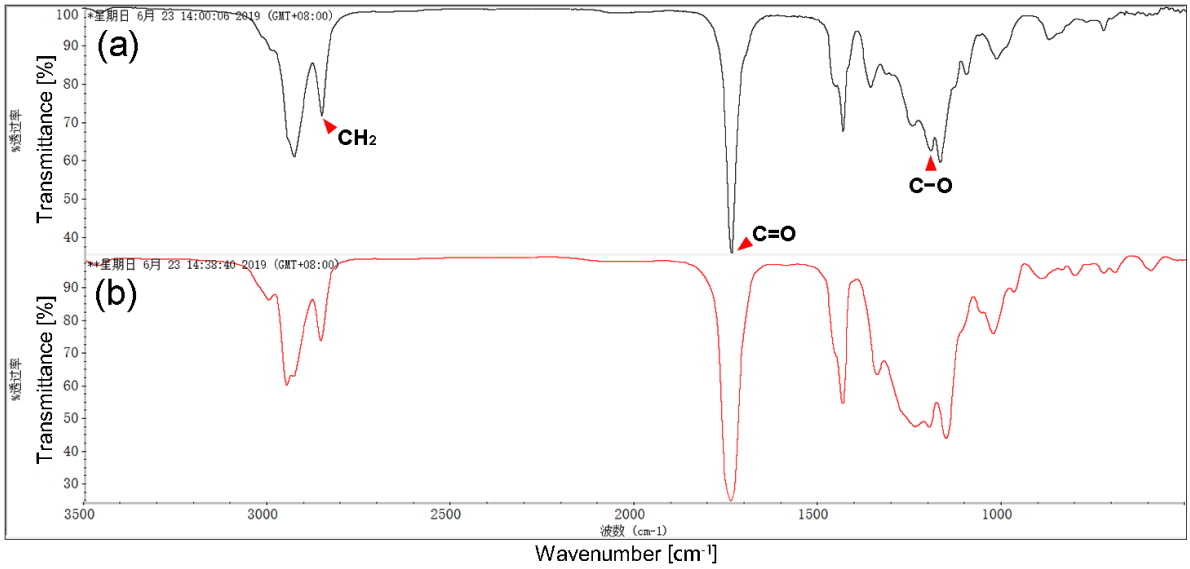

Figure S4. FT-IR spectra of (a) DMS and (b) EB-DMS. Relative to DMS, the absorption intensity ratios of carbonyl (1740 cm^{-1}) and C-O (1197 cm^{-1}) stretching to that of methylene (2857 cm^{-1}) increased from 3.00 and 1.38 to 4.43 and 2.36, respectively, after Claisen condensation. The rationale behind the selection of methylene as the internal standard for quantitative comparison was based on the fact that they remained stoichiometrically consistent throughout the functionalization procedure.

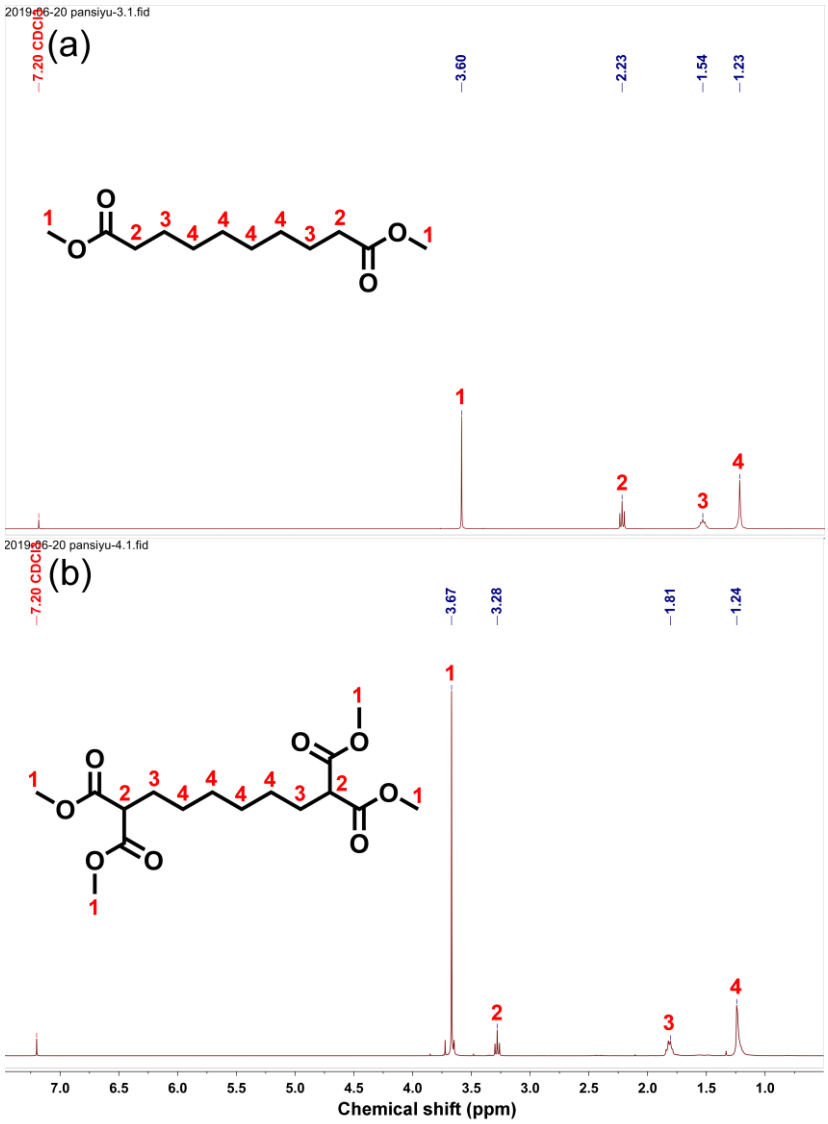

Figure S5. ^{1}H NMR spectra of (a) DMS and (b) EB-DMS. Relative to the signal corresponding to methylene protons (**4**) whose position and integral remained constant before and after Claisen condensation, the integral under the methoxy resonance signal (**1**) doubled in EB-DMS, suggesting those extra methyl esters were in stoichiometric quantities. One could surmise that the ester branch was covalently attached at the α-position of the feedstock, given the integral under the α-proton signal (**2**) was halved after Claisen condensation. Meanwhile, the attached ester thinned the electron clouds on adjacent protons, and hence the resonance position of the α- (**2**) and β-protons (**3**) shifted downfield from 2.2 and 1.5 to 3.3 and 1.8 ppm, respectively.

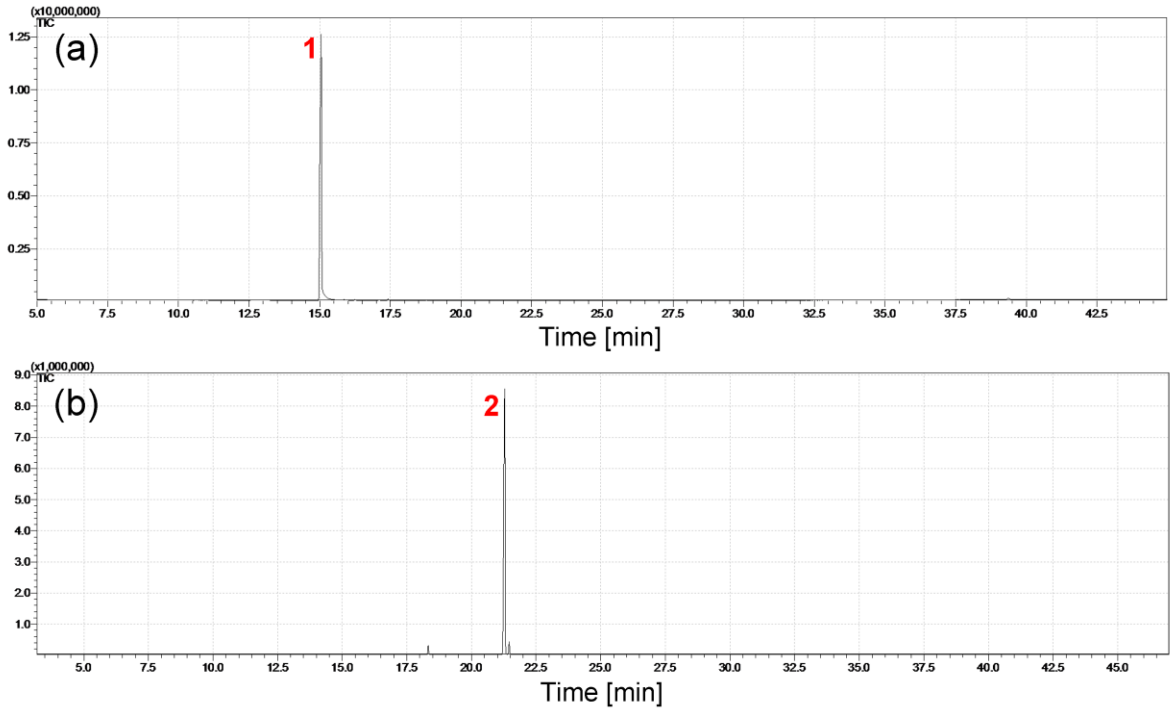

Figure S6. Gas chromatograms of (a) DMS and (b) EB-DMS.

Table. S2 Composition of each gas chromatogram peak in Figure S6 as identified by comparing their recorded mass spectra against NIST08 Mass Spectral Library.

Peak	Retention time (min)	Composition	Molecular formula	Area (%)		Matching degree (%)
				Feedstock	Product	
1	15.1	Dimethyl sebacate	$C_{12}H_{22}O_4$	99.2		95
2	21.3	Ester-branched dimethyl sebacate	$C_{16}H_{26}O_8$		95.2	n/a[a]
		Other compounds	n/a	0.8	4.8	n/a

[a] Component **2** could not be explicitly identified by NIST08 Mass Spectral Library, but its structure could be inferred from its retention time and peak area in Figure S6, characteristic fragment ions in the recorded mass spectra (Figure S11, *m/z* 132 and 145 corresponding to dimethyl malonate and dimethyl methylmalonate anionics, respectively), and composition of the feedstock.

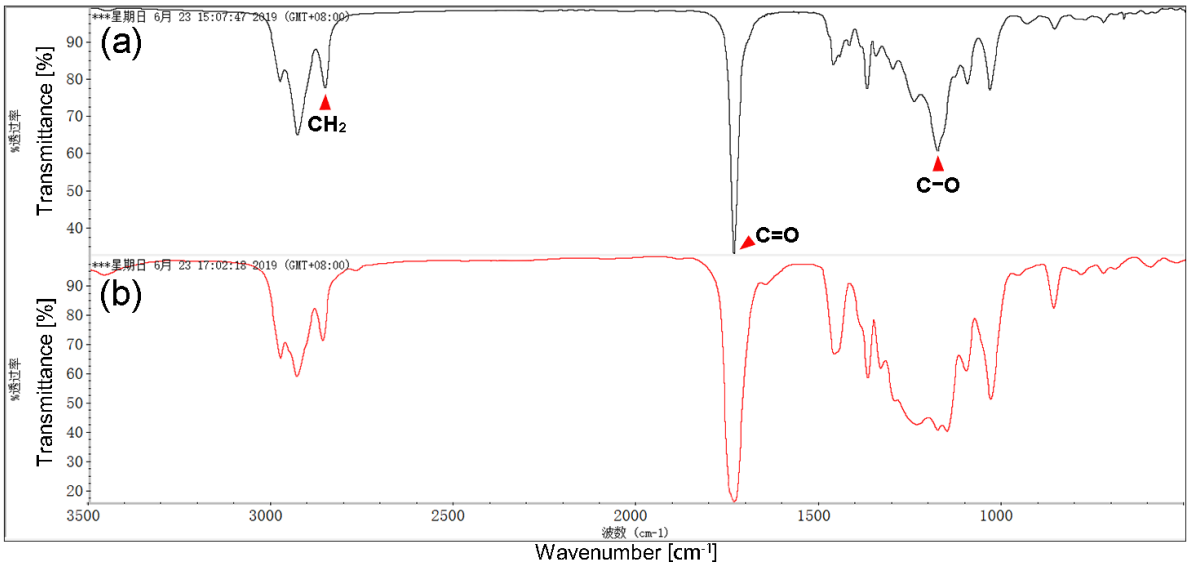

Figure S7. FT-IR spectra of (a) DES and (b) EB-DES. Relative to DES, the absorption intensity ratios of carbonyl (1736 cm^{-1}) and C-O (1180 cm^{-1}) stretching to that of methylene (2857 cm^{-1}) increased from 4.33 and 1.89 to 5.90 and 2.87, respectively, after Claisen condensation. The rationale behind the selection of methylene as the internal standard for quantitative comparison was based on the fact that they remained stoichiometrically consistent throughout the functionalization procedure.

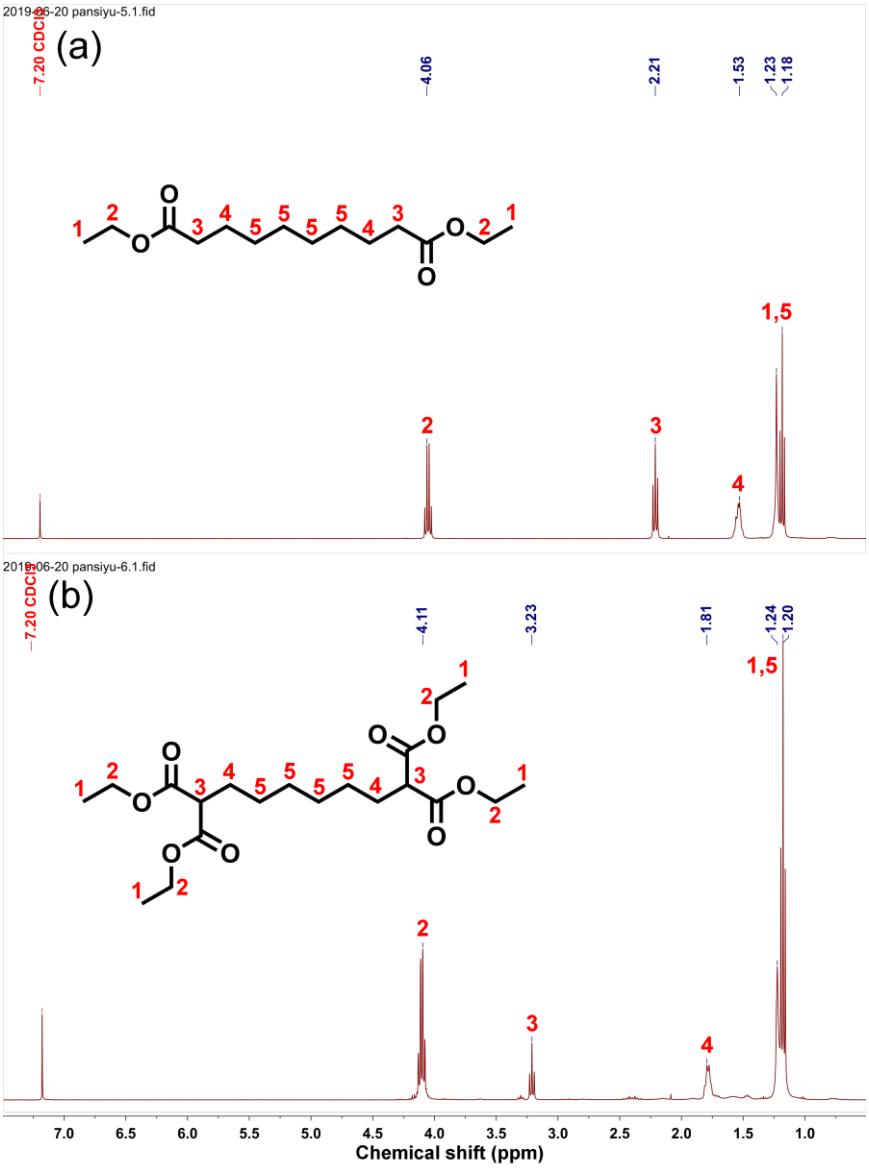

Figure S8. ^{1}H NMR spectra of (a) DES and (b) EB-DES. Relative to the signal corresponding to methylene protons (**4**) whose position and integral remained constant before and after Claisen condensation, the integral under the alkoxy resonance signal (**2**) doubled in EB-DES, suggesting those extra ethyl esters were in stoichiometric quantities. One could surmise that the ester branch was covalently attached at the α-position of the feedstock, given the integral under the α-proton signal (**3**) was halved after Claisen condensation. Meanwhile, the attached ester thinned the electron clouds on adjacent protons, and hence the resonance position of the α- (**3**) and β-protons (**4**) shifted downfield from 2.2 and 1.5 to 3.2 and 1.8 ppm, respectively.

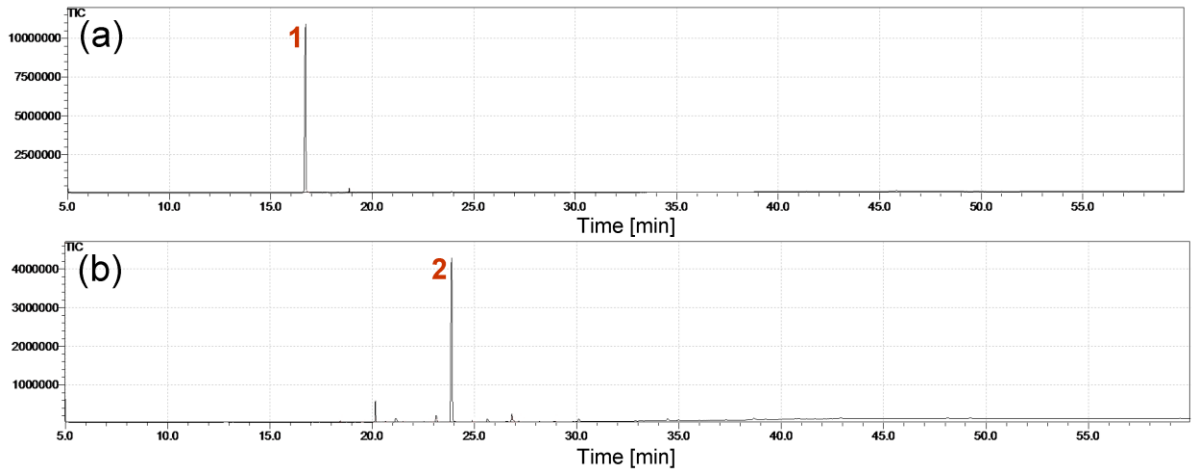

Figure S9. Gas chromatograms of (a) DES and (b) EB-DES.

Table S3. Composition of each gas chromatogram peak in Figure S9 as identified by comparing their recorded mass spectra against NIST08 Mass Spectral Library.

Peak	Retention time (min)	Composition	Molecular formula	Area (%)		Matching degree (%)
				Feedstock	Product	
1	16.7	Diethyl sebacate	$C_{14}H_{26}O_4$	98.5		96
2	23.7	Ester-branched diethyl sebacate	$C_{20}H_{34}O_8$		89.2	n/a[a]
		Other compounds	n/a	1.5	10.8	n/a

[a] Component **2** could not be explicitly identified by NIST08 Mass Spectral Library, but its structure could be inferred from its retention time and peak area in Figure S9, characteristic fragment ions in the recorded mass spectra (Figure S12, *m/z* 160 and 173 corresponding to diethyl malonate and diethyl methylmalonate anionics, respectively), and composition of the feedstock.

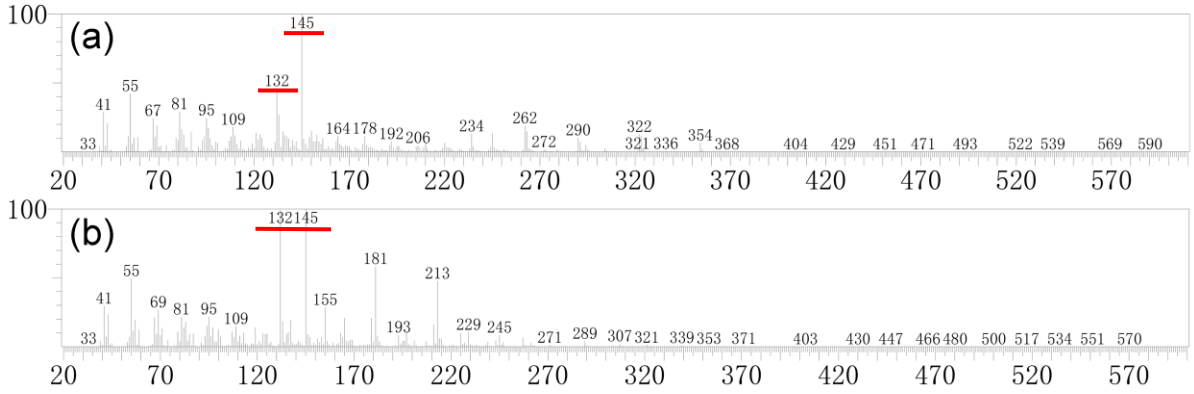

Figure S10. Mass spectra of (a) component **3** and (b) component **5** in Figure 3. The characteristic fragment ions with *m/z* 132 and 145 corresponded to dimethyl malonate and dimethyl methylmalonate anionics, respectively.

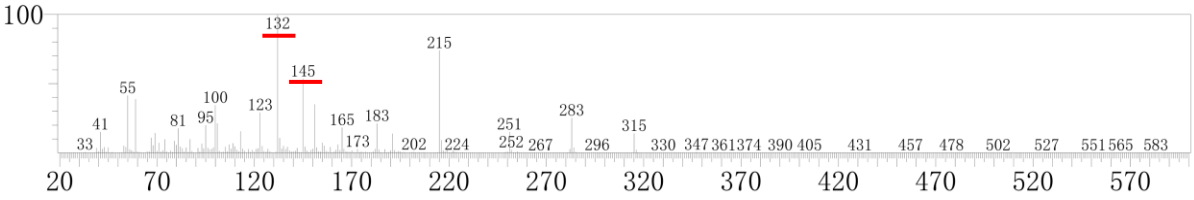

Figure S11. Mass spectrum of component **2** in Figure S6. The characteristic fragment ions with *m/z* 132 and 145 corresponded to dimethyl malonate and dimethyl methylmalonate anionics, respectively.

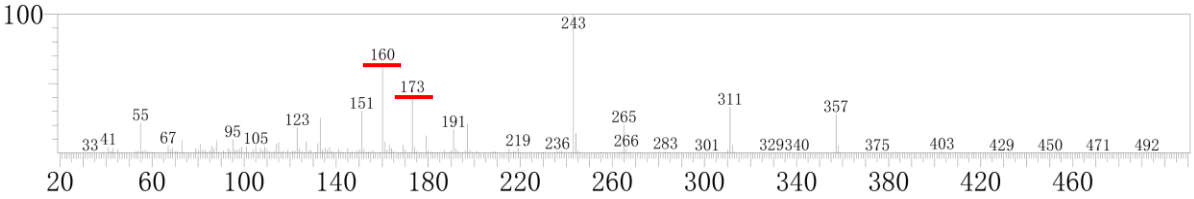

Figure S12. Mass spectrum of component **2** in Figure S9. The characteristic fragment ions with *m/z* 160 and 173 corresponded to diethyl malonate and diethyl methylmalonate anionics, respectively.

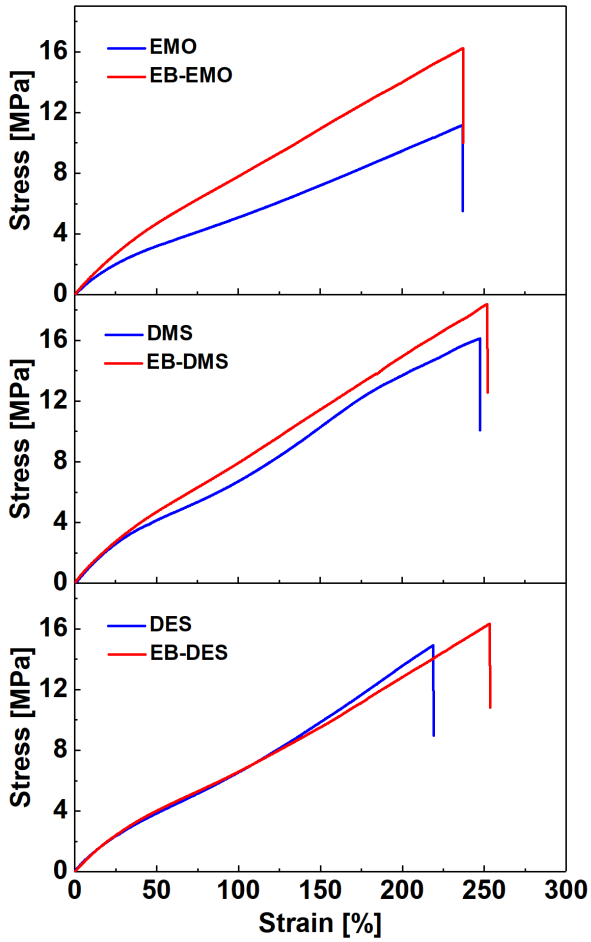

Figure S13. Stress-strain curves of PVC membranes containing ester-branched and the parent plasticizers.

Table S4. Simulated and experimental density (ρ), cohesive energy density (CED), and Hildebrand solubility parameter (σ) of the pure PVC model, well-equilibrated at 300 K after simulated annealing.

	ρ (g/cm^3)	CED $\times 10^8$ (J/m^3)	σ ($(J/cm^3)^{0.5}$)
Simulated	1.381±0.003	3.85±0.05	19.52±0.14
Experimental	1.38-1.41[1,2]	3.76-3.92[3]	19.39-19.80[3]

References

1. Alexander G. J. Driedger, Hans H. Dürr, Kristen Mitchell, Philippe Van Cappellen. Plastic debris in the laurentian great lakes: a review. Journal of Great Lakes Research, 2015, 41: 9-19.
2. Zhonglin Luo, Jianwen Jiang. Molecular dynamics and dissipative particle dynamics simulations for the miscibility of poly(ethylene oxide)/poly(vinyl chloride) blends. Polymer, 2010, 51: 291-299.
3. Irving Skeist. Handbook of adhesives. Springer Science & Business Media, 2012.